A study of shallow crustal structure in the Mygdonia Basin (N. Greece) based on the dispersion curves of Rayleigh waves

E.E. Karagianni *, D.G. Panagiotopoulos*, C.B. Papazachos**, and P.W. Burton***

* Geophysical Laboratory, University of Thessaloniki, Thessaloniki, Greece, GR- 54006.
** Institute of Engineering Seismology and Earthquake Engineering
Georg.Scholis 46, P.O. Box 53, GR-55102 Finikas, Thessaloniki, Greece.
*** University of East Anglia, School of Environmental Sciences, Norwich NR4 7TJ, U.K.

Abstract : *A big shot experiment was carried out in the Mygdonia basin during the project "EUROSEISTEST VOLVI-THESSALONIKI, a European test site for Engineering Seismology, Earthquake and Seismology". This experiment was realised by using an explosion of 75 kg of explosives placed at 20 m depth. The aim of the explosion was to investigate the geometry and the V_S profile across the valley, between the villages Profitis and Stivos which are laid between the lakes Koronia (Lagada) and Volvi in Northern Greece. The records of Rayleigh waves as they were generated by the big shot and recorded on the vertical components of the portable stations which were installed in Mygdonia basin, were analysed in order to obtain the group velocity dispersion curves corresponding to propagation paths between the shot point and the recording stations. Furthermore, these dispersion curves were inverted to determine the shear wave velocity models along the propagation paths by using linear approach.*
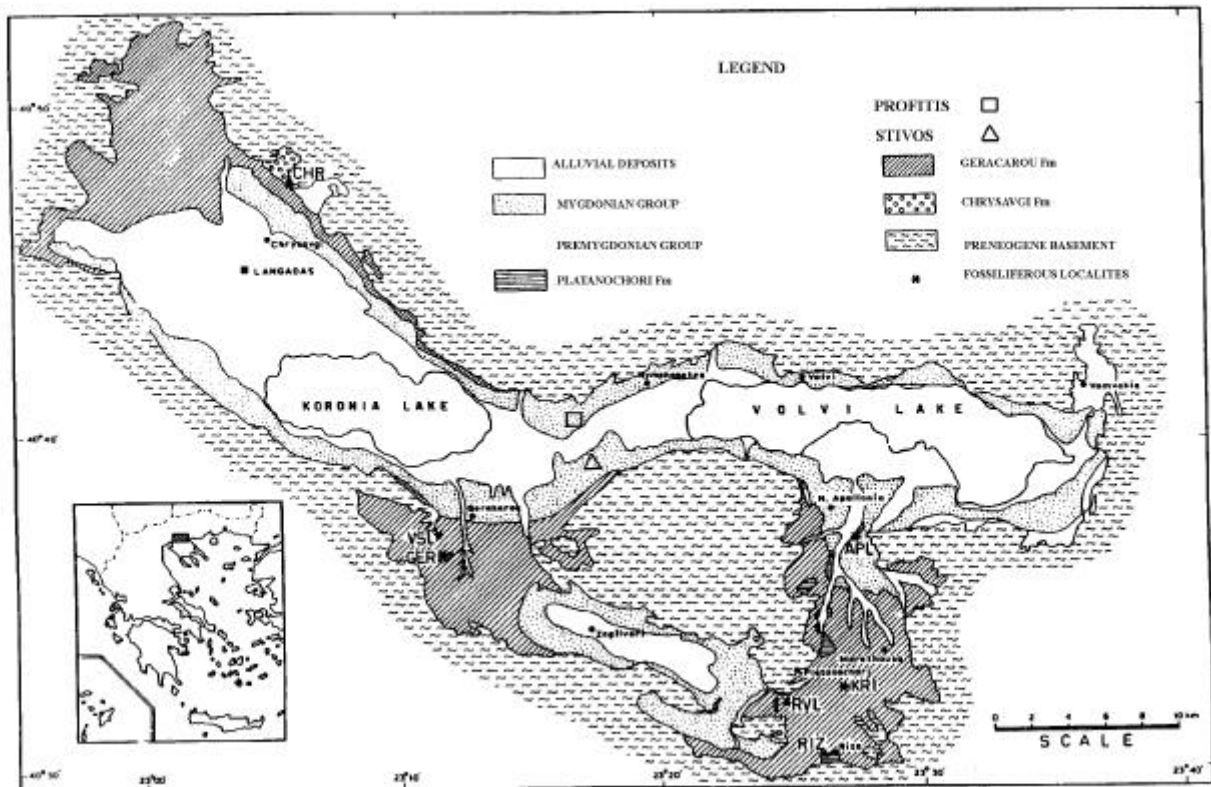
INTRODUCTION

Mygdonia basin is one of the most active seismic zones in Northern Greece and the surrounding area. It is located in the northern part of Aegean region where two major tectonic phenomena are observed: a) the extension of the Aegean region in an approximate N-S direction and b) the termination of the North Anatolian strike slip fault. Seismological and geological research suggest that this extension to be the basic reason for the shallow earthquakes in the Aegean Sea, Continental Greece and in the Western Turkey (McKenzie, 1972, 1978; Ritsema, 1974; Papazachos and Comninakis, 1976; Mercier, 1977).

From a geological point of view, the valley of Mygdonia is located at the border area of two geotectonic zones in Greece, namely the Servomacedonian massif and the zone of Axios. A series of grabens with E-W to NW-SE trends were formed by normal faulting in the area of the Servomacedonian massif during the Neogene and Quaternary. The Mygdonia basin is the remnant of one of these grabens. The basement of Mygdonia basin consists of gneiss with several marble bands interbedded between of amphiboles, limestones, quartzites or phyllites. Mygdonia basins, as well as other smaller surrounding basins (Marathousa, Vromolimnes, Doubia, and Zagliveri) are the remnants of an initial older basin named Premygdonian basin (Fig. 1).

During Neogene-early Pleistocene, the Premygdonia basin was filled by fluvioterrestrial and lacustrine sediments, which consisted of the Premygdonia group with a thickness reaching 350-400 m. At the end of early Pleistocene a new phase of tectonic action faulted the Premygdonian basin resulting in smaller basins like Marathousa, Vromolimnes, Doubia, Zagliveri to be formed. These new grabens occurred in an E-W direction. The Mygdonia basin is being the largest among these new basins. It was filled with water forming the large Mygdonia lake. The present lakes Volvi and Lagada (Koronia) are the remnants of the previous Mygdonia lake.

The Mygdonia basin is filled up by sedimentary deposits, which can be distinguished in the lower unit "Premygdonia system" and the upper unit "Mygdonia system". The "Premygdonia system" consists of four

FIG. 1. Geological map of Neogene-Quaternary deposits of Mygdonia Basin (Koufos *et al.*, 1995).
(At the rectangle defines the region of study).

different formations, namely conglomerates, sand-stone, silt/sand sediments and red beds, which were deposited in subsided Premygdonian basin during the Neogene. The Mygdonia system consists of various types of sediments, and is the youngest graben in the tectonically differentiated Premygdonia basin during the Quaternary. These sediments contain alluvial, fluviolacustrine, deltaic, lacustrine and lagoonal (Psilovikos 1977; Psilovikos et al. 1983).
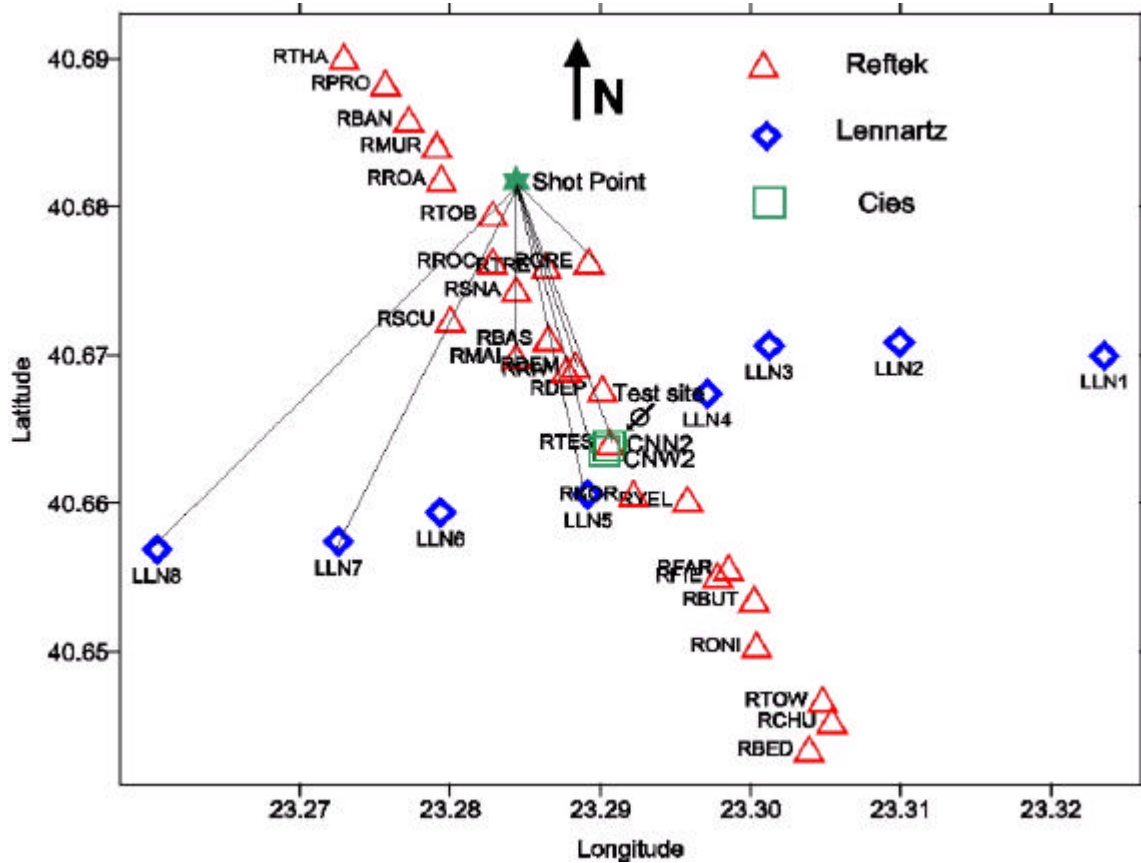
In view of the most recent studies, the stress field in Mygdonia graben is dominated by a horizontal tensional stress field striking in a NNW-SSE direction (McKenzie 1978; Le Pichon and Angelier, 1979; Papazachos et al., 1980, 1984; Soufleris et al., 1982; Scordilis, 1985). The NNW-SSE extension is in agreement with the in-situ measurements of principal stress (Paquin et. al., 1981). Moreover, the normal Neogene faults which were observed in Mygdonia graben after the big earthquake of 20th June 1978 near Thessaloniki are in accordance with the N-S extension in Mygdonia basin (Faugeres, 1975; Psilovikos, 1977; Mercier, 1977).

During the project "EUROSEISTEST VOLVI-THESSALONIKI, a European test site for Enginee-ring Seismology, Earthquake and Seismology", five different techniques were employed (P- and S- wave refraction tests, inversion of surface waves, borehole tests, reflection and tube wave analysis) in order to determine a velocity cross-section across the valley

between the villages Profitis and Stivos. The results of all these techniques were used and six different layers were identified along the cross-section with the velocities of P waves ranging from 375 m/sec for the upper layers to 4500 m/sec for the weathered bedrock, and the velocities of S waves ranging from 225 to 2600 m/sec for the upper layers and the weathered bedrock, respectively (Final Scientific report of EUROSEISTEST). Furthermore, the depth of meta-morphic basement is determined as about 250 m by the seismic survey and of about 350 m by the electric survey. In addition AUTh.GL (Aristotle University of Thessaloniki, Geophysical Laboratory, Thessaloniki, Greece), LGIT-OG (Laboratoire de Geophysique Interne & Tectonophy-sique, Observatoire de Grenoble, France) and AUTh.SF (Aristotle University of Thessaloniki, Laboratory of Soil Mechanics and Foundation Engineering) performed a big shot experiment in order to study the geometry and V$_S$ profile across the valley between Profitis and Stivos.

DATA AND DISPERSION ANALYSIS

The data used in this study obtained from the shot experiment that was performed by AUTh.SF, LGITOG and AUTh.GL during the project "EUROSEISTEST". The explosion was performed on August 12th, 1994 with 75 Kg of explosives at a depth of 20 m.

FIG. 2. The portable recording stations (Reftek, Lennartz and Cies arrays) and the position of the shot point.

During the aforementioned project four (4) types of portable recording stations were used: Reftek, Lennartz, Cies and Tad. In figure 2 the sites of Reftek, Lennartz and Cies, as well as the position of the shot point are shown.
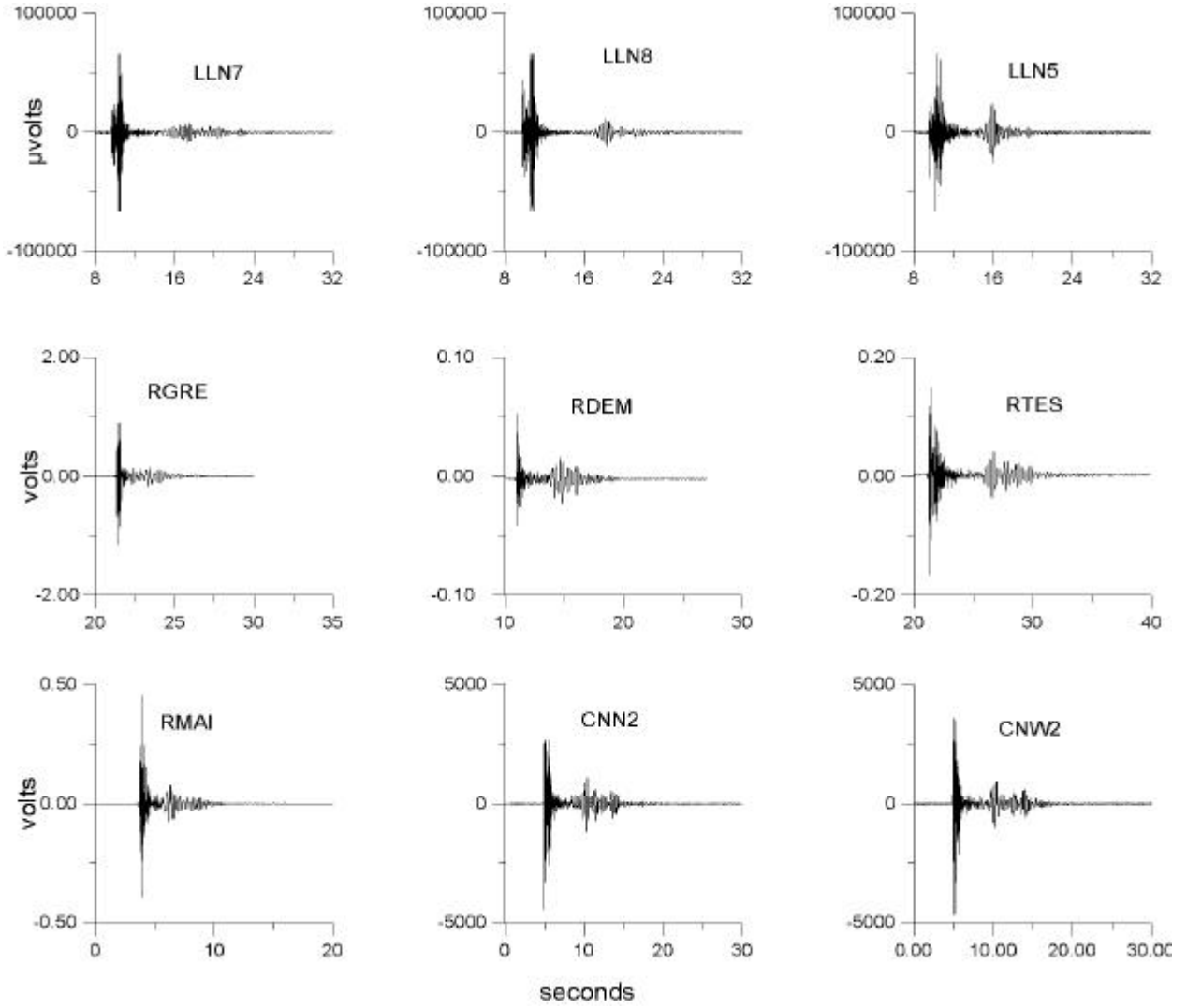
The Reftek network (Fig. 2) consisted of 23 recording stations installed along a NNW-SSE profile between Profitis and Stivos. 18 of these stations have capability of measuring 6-component traces by using two 3D sensors, and have additionally one sensitive velocimeter and one accelerometer. Stations with different velocity sensors were also used. Most of them were 2 Hz velocimeters (Mark-L22). Moreover, 7 CMG40 sensors were installed, which have a flat response above a frequency of 0.05 Hz. The Lennartz network consisted of 8 Mars88 stations installed along an E-W line, parallel to the valley axis and crossing the Reftek array (Fig. 2). The total length of this line was 5 Km and the spacing between the stations ranged from 500 m to 1 Km. The Cies network consisted of 8 stations equipped with 5s 3D velocimeters installed very close to each other.

The Rayleigh waves generated by the big shot were recorded on the vertical components of the portable recording stations and used in order to estimate the variation of the seismic shear wave velocity as a function of depth along various propagation paths. The records of the explosion had a sampling interval of 0.008 sec for Lennartz and 0.01 sec for Reftek and Cies stations.

Not all the explosion records were used because some of the stations exhibited large noise levels. Figure 2 illustrates the seismic ray paths between the shot point and the stations used and the recorded Rayleigh waves data for the vertical-components of Lennartz, Reftek and Cies stations are shown in Figure 3.

The data were first analysed with multiple filter technique (Dziewonski et. al., 1969). For each record between the shot point and the recording stations, the group velocity dispersion curve of Rayleigh waves was calculated using the program TSAP (Time Series Analysis Program) (Burton and Blamey, 1972). The observed dispersion curves were calculated for a long frequency window allowing the determination of the dispersion curves that are useful for frequencies between 1-6 Hz for Lennartz and Cies, and 2-7 Hz for Reftek stations due to the poor signal content for lower frequencies and scattering effects at higher frequencies. Frequencies lower than the eigenfrequencies of the instruments were not used and the instrument response was not considered.

FIG. 3. The Rayleigh waves records (vertical components) from the portable Lennartz, Reftek and Cies stations.

In Figure 4 the observed dispersion curves for each propagation path are illustrated, with the corresponding error for each value of group velocity.

LINEAR INVERSION OF SURFACE WAVES

Each dispersion curve of the group velocity of Rayleigh waves corresponding to the different propagation paths between the shot point and recording stations was inverted using the linear inversion scheme (Backus and Gilbert, 1967, 1968, 1970; Wiggins, 1972). A very brief description of the linear inversion method is given below (Braile and Keller, 1975).

The basic equation for the general linear inverse problem is:

$$y=Ax \tag{1}$$

where the observations **y** are related to the model **x** by the data kernel **A**. If a non-linear problem is assumed to be linearised in the neighbourhood of the solution, then **y** becomes the difference between the observed and theoretical data which are calculated from an initial model x_0. **x** denotes the parameter change vector which must be added to the initial model x_0
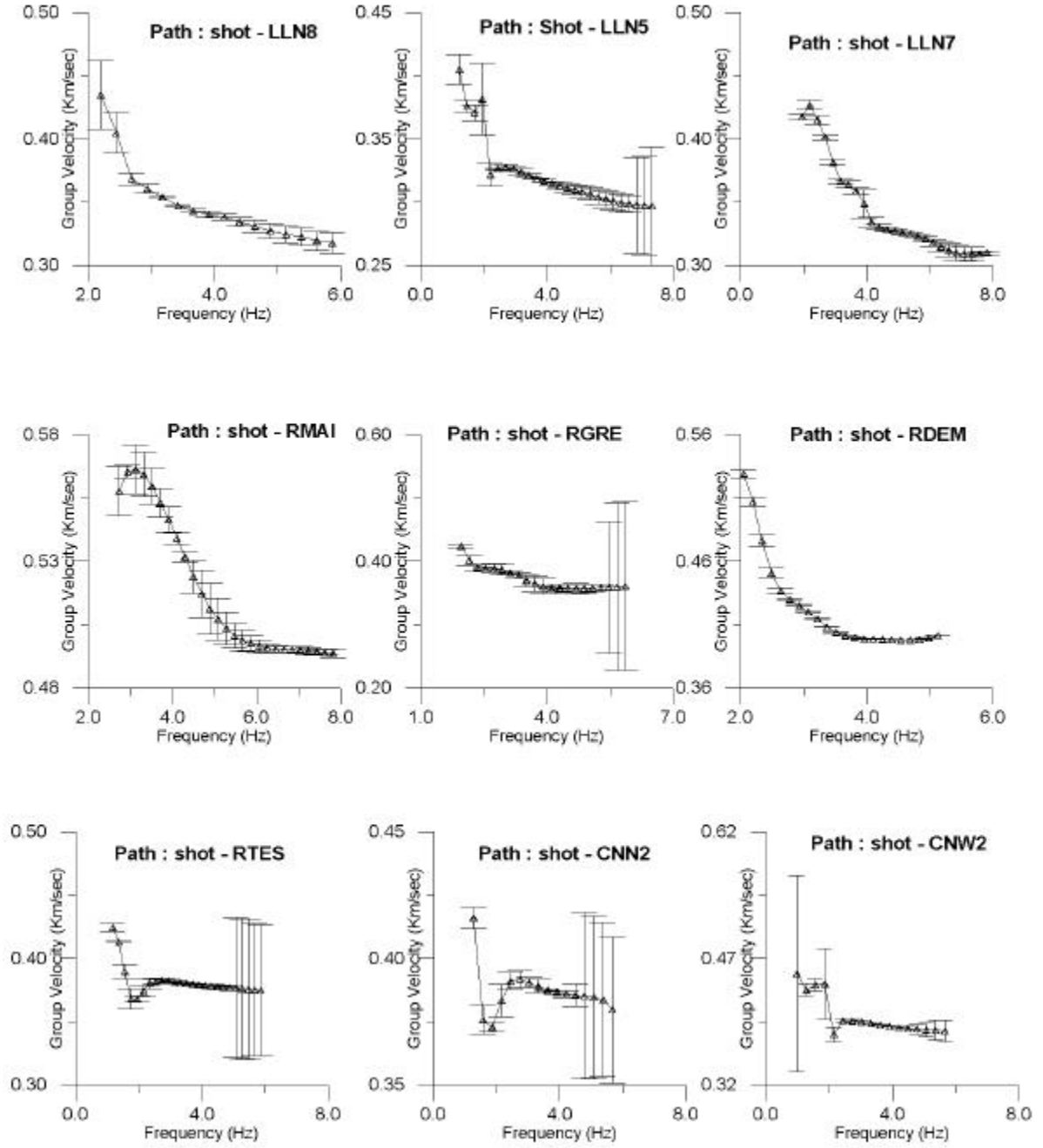
and are to be determined by the minimisation of **y**. The data kernel matrix (**A**) becomes the matrix of partial derivatives which are the first order Taylor series expansions of the nonlinear functional about the initial model x_0, and it is called the Jacobian matrix of a non-linear problem.

In general the matrix **A** is nonsquare, hence we seek a solution or model $\hat{x}$ by operating on (1) with a generalized inverse matrix **H**:

$$\hat{x} \equiv HAx = Hy \tag{2}$$

A is decomposed into the multiplication of three orthogonal matrixes, $H = V\Lambda^{-1}U^T$ (Lanczos, 1961) where the columns of **V** are eigenvectors associated with the columns of **A**, the rows of U^T are eigenvectors associated with the rows of **A** and Λ^{-1} is a diagonal matrix whose diagonal elements are reciprocals of the eigenvalues of **A**.

If the number of observations is greater than the number of parameters then the generalised inverse is given by the equation $H_{LS} = \left(A^TA\right)^{-1}A^T$ and the vector of parameter changes is given by equation

FIG. 4. Observed dispersion curves of Rayleigh waves group velocity for different propagation
paths with the corresponding standard error for each value of group velocity.

$\hat{\mathbf{x}} = \left(\mathbf{A}^{\mathbf{T}}\mathbf{A}\right)^{\mathbf{-1}}\mathbf{A}^{\mathbf{T}}\mathbf{y}$ which is equivalent to the classical least squares inverse. For the case where the number of parameters is greater than the number of observations, the generalised inverse matrix is given by the equation $\mathbf{H} = \mathbf{A}^{\mathbf{T}}\left(\mathbf{AA}^{\mathbf{T}}\right)^{\mathbf{-1}}$, which has been applied to geophysical problems by Smith and Franklin (1969).

From equation (2) it is obvious that the product matrix **HA**, which is known as resolution matrix **R**, maps the entire set of possible solution **x** into a single model $\hat{\mathbf{x}}$ (Backus and Gilbert, 1968). The degree to which the matrix **R** approximates an identity matrix is a measure of the resolution of the model. Therefore, if

R is an identity matrix, then $\hat{\mathbf{x}}$ is the unique solution of equation (1). Rows of **R** are known as averaging resolving kernels. An estimation of the variance of the model operating by equation (2) is given by the following equation (Jackson, 1972)

$$\mathrm{var}\,\hat{\mathrm{x}}_{\mathrm{k}} = \sum_{j=1}^{p}\left(V_{kj}/\lambda_{j}\right)^{2} \qquad (3)$$

where p is the number of nonzero eigenvalues λ_{j} of matrix **A**, which are used for the calculation of matrix **H**. Because the eigenvalues appear in the denominator of (3), the variance of the model will take unacceptable large values for small eigenvalues.

Table 1. Final models of shear wave velocity with the thickness of the layers for each propagation path.

Shot-LLN7

S-Velocity	Thickness
(Km/sec)	*(Km)*
0.3227	0.010
0.4154	0.015
0.4518	0.020
0.5343	0.000

Shot-LLN8

S-velocity	Thickness
(Km/sec)	*(Km)*
0.2326	0.010
0.5828	0.010
0.4129	0.015
0.4642	0.000

Shot-LLN5

S-velocity	Thickness
(Km/sec)	*(Km)*
0.3478	0.025
0.4223	0.030
0.4358	0.030
0.5393	0.000

Shot-RDEM

S-velocity	Thickness
(Km/sec)	*(Km)*
0.4711	0.025
0.5038	0.025
0.6064	0.035
0.7151	0.000

Shot-RGRE

S-velocity	Thickness
(Km/sec)	*(Km)*
0.4264	0.020
0.3791	0.015
0.4823	0.000

Shot-RMAI

S-velocity	Thickness
(Km/sec)	*(Km)*
0.5637	0.020
0.5769	0.020
0.6731	0.000

Shot-RTES

S-velocity	Thickness
(Km/sec)	*(Km)*
0.4180	0.035
0.4685	0.035
0.4542	0.035
0.5741	0.000

Shot-CNN2

S-velocity	Thickness
(Km/sec)	*(Km)*
0.4157	0.035
0.4814	0.045
0.3479	0.015
0.5692	0.000

Shot-CNW2

S-velocity	Thickness
(Km/sec)	*(Km)*
0.4323	0.040
0.4927	0.040
0.3937	0.010
0.5486	0.000

In order to eliminate the "near-zero" eigenvalues and the associated eigenvectors from the matrices $\mathbf{V}$ and $\mathbf{U^T}$ for the calculation of the matrix H, two methods were used. One method is to use a cut-off strategy (Lanczos, 1961), where we consider a critical value λ_c and all the eigenvalues less than λ_c are regarded to be practically zero. This reduces the variance estimates given by equation (3) but degrades the resolution matrix, $\mathbf{R}$. Choosing a suitable critical value for λ_c effects a trade off between resolution and variance of the model.

A second approach is to damp an unstable inversion, called the Levenberg-Marquadt method (Levenberg, 1944; Marquadt, 1963). In this case the generalized inverse matrix is given by the equation $\mathbf{H_{LM}} = \mathbf{VMU^T}$, where the matrices $\mathbf{V}$, $\mathbf{U^T}$ are the same as in least-squares approach and the matrix $\mathbf{M}$ is a diagonal matrix of elements m_i given by the following equation:
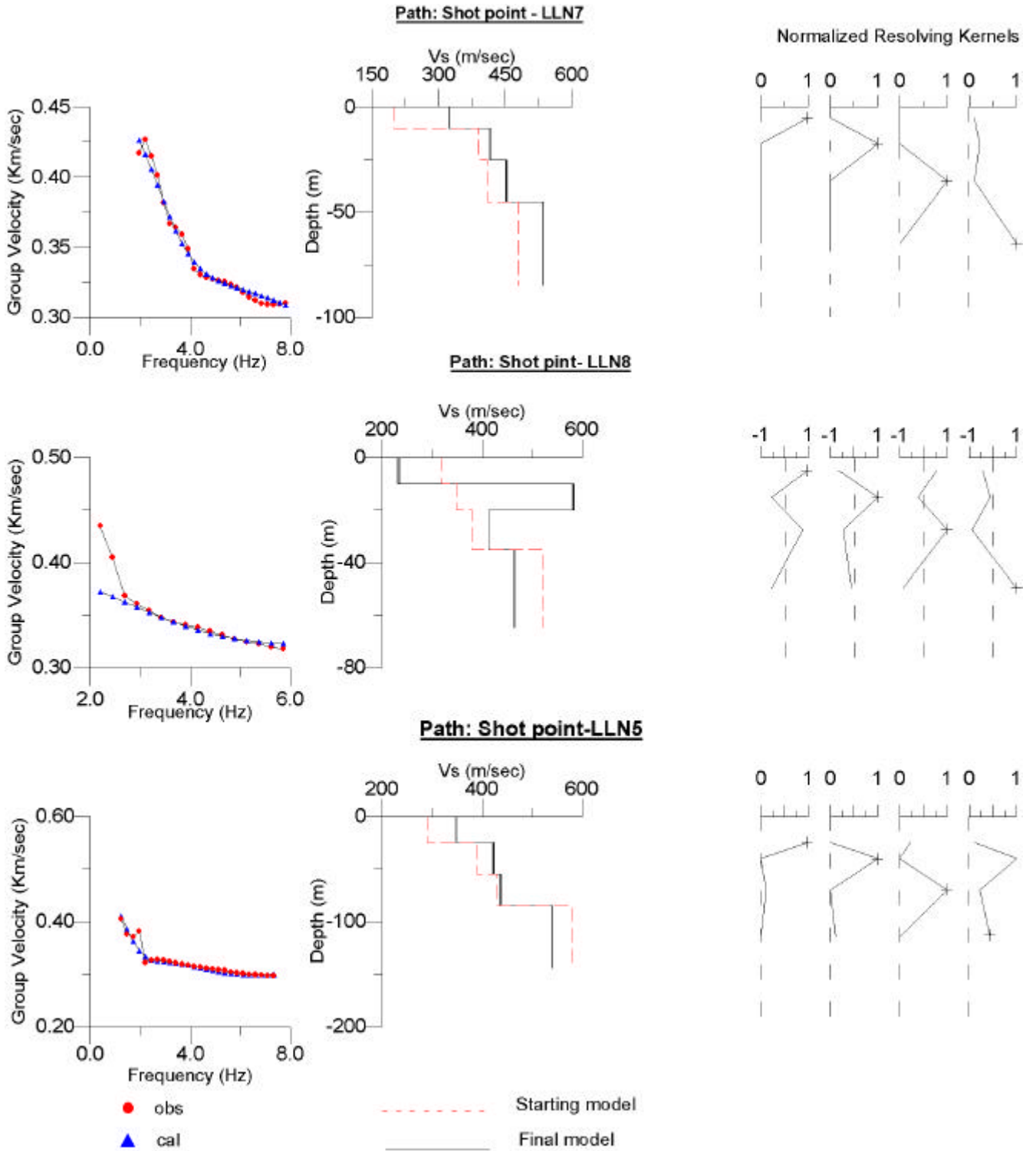
$$m_i = \frac{\lambda_i}{\lambda_i + \Theta} \qquad i = 1, p \qquad (4)$$

and the vector of parameter changes for the derived model becomes:

$$\hat{\mathbf{x}} = \left(\mathbf{A^T A} + \Theta\mathbf{I}\right)^{-1}\mathbf{A^T y} \qquad (5)$$

The parameter Θ, is known as damping factor of Levenberg-Marquadt. Adding the damping factor to the main diagonal of the matrix $\mathbf{A^T A}$, the values of small eigenvalues are increased in order to eliminate zero eigenvalues, thus leading to a stable inversion of $\left(\mathbf{A^T A} + \Theta\mathbf{I}\right)$. The choice of the damping factor Θ must combine good resolution and minimization of 'near-zero' eigenvalues.

In this study, a damped least-squares matrix procedure is applied by using the Levenberg-Marquardt parameter for the dispersion curves (of fundamental mode of group velocity for the Rayleigh waves for the different paths) to derive the variations of shear wave velocity versus depth. A starting model of shear wave velocity versus depth is used in order to calculate a theoretical dispersion curve that fit the observed one. The starting models proposed by previous investigations were used (Final Scientific report of EUROSEISTEST). The theoretical dispersion curves are calculated using the Thomson-Haskel technique (Thomson, 1950; Haskell, 1953) as it has been modified by Schwab and Knopoff (1972). In this algorithm the Poisson ratio was set equal to 0.26 (Scordilis, 1985) which gave the relationship

FIG. 5. Shear wave velocity versus depth profile along the propagation paths between shot point and Lennartz stations. For each model the resolving kernels and the fit between observed and theoretical dispersion curve are presented.

$\alpha = 1.77\beta$ between the longitudinal and shear wave velocities. The relationship between density and shear wave velocity given by Keller et al. (1976) was also used. Using a starting model of shear wave velocity versus depth for each propagation path a theoretical dispersion curve of group velocity was calculated using the Thomson-Haskel technique. Moreover, for the starting model, the partial derivative matrix **A** of

equation **y=Ax**, is calculated in order to connect the small variations of group velocity with the small variations in the model parameters. This procedure is repeated iteratively until a satisfactory agreement between the theoretical and measured data is obtained. The model that provides the best fit between the observed and theoretical dispersion curves is considered as the best model for the area under study.

RESULTS AND DISCUSSION

In Table 1, the final models of shear wave velocity for each propagation path are presented. The results of linear inversion scheme for each path are shown in Figures 5, 6 and 7. Each of these figures presents:

- The fit between observed and theoretical dispersion curves (the circles correspond to the observed value of group velocity and the triangle to the calculated value of group velocity).

- The graph of starting and final models of shear wave velocities versus depth. For the final model, the value of shear velocity together with its standard error for each layer and the underlying halfspace are shown.

- The resolving kernels. A resolving kernel for each layer and the halfspace was drawn. The surface layer is presented by the first to the left resolving kernel and the halfspace from the first to the right kernel. The resolving kernel with a narrow positive peak, at its own layer depth, shows that the layer is well resolved, while a broad peak implies a poor resolution. In the graph of resolving kernels the dashed line gives the zero line for reference.

From the graphs of the final models the results for each propagation path can be summarised:

- For the path between the shot point and LLN7, the starting model consisted of three layers, reaching a depth of 45 m, and a halfspace. For this path there is a very good fitness between observed and theoretical dispersion curve, with a very good resolution of resolving kernels. The final model shows a continuous increase of shear wave velocity with depth.

- For the path between shot point and LLN8, the starting model consisted of three layers reaching a depth of 35 m and a halfspace. The final model presents a low velocity layer in a depth of 30 m.

- For the path between the shot point and LLN5, the starting model consisted of three layers reaching a depth of 85 m, and a halfspace. The final model presents a continuous increase of shear wave velocity versus depth, with a very good resolution of the resolving kernels peaking at the depth of the corresponding layers for depths less than 85 m, while at larger depths, the maximum is considerably at shallower depths.

- For the path between the shot point and RDEM, the starting model consisted of three layers reaching a depth of 85 m and a halfspace. The final model shows a continuous increase of shear wave velocity with depth, with a good fit between observed and theoretical dispersion curves and also a good resolution of resolving kernels.

- For the path between the shot point and RMAI, the starting model consisted of two layers reaching a depth of 40 m, and a halfspace. The final model presents a good fit of theoretical and observed dispersion curves with a good resolution of resolving kernels.

- For the path between the shot point and RGRE, the starting model consisted of two layers reaching a depth of 35 m, and a halfspace. The final model presents a low velocity layer at a depth of 30-35 m.

- The stations RTES, CNN2 and CNW2 are located very close to each other and the linear inversion scheme for these paths shows a low velocity layer at a depth of 90-100 m. Moreover, a low velocity layer has been found near to the sites of previous stations from refraction and reflection tests but at a smaller depth.

Using the final models of shear waves velocity versus depth for the different paths, the section was reconstructed and illustrated in Figure 8. The section has a NNW-SSE direction that is perpendicular to the principal axis of the Mygdonia basin. This is why only the results from Reftek and Cies stations were used, because they were installed in the same direction. For each propagation path, each model was considered in the middle of the distance between the shot point and the recording stations. So in Figure 8 the triangles correspond to the sites of shot point and stations, the names of the stations with capital letters show the sites of these stations and the names of the stations with the small letters correspond to the middle of the distance between the shot point and each of the corresponding stations.

In order to group the values of shear wave velocity, it was supposed that three stratigraphic sequences were existed:
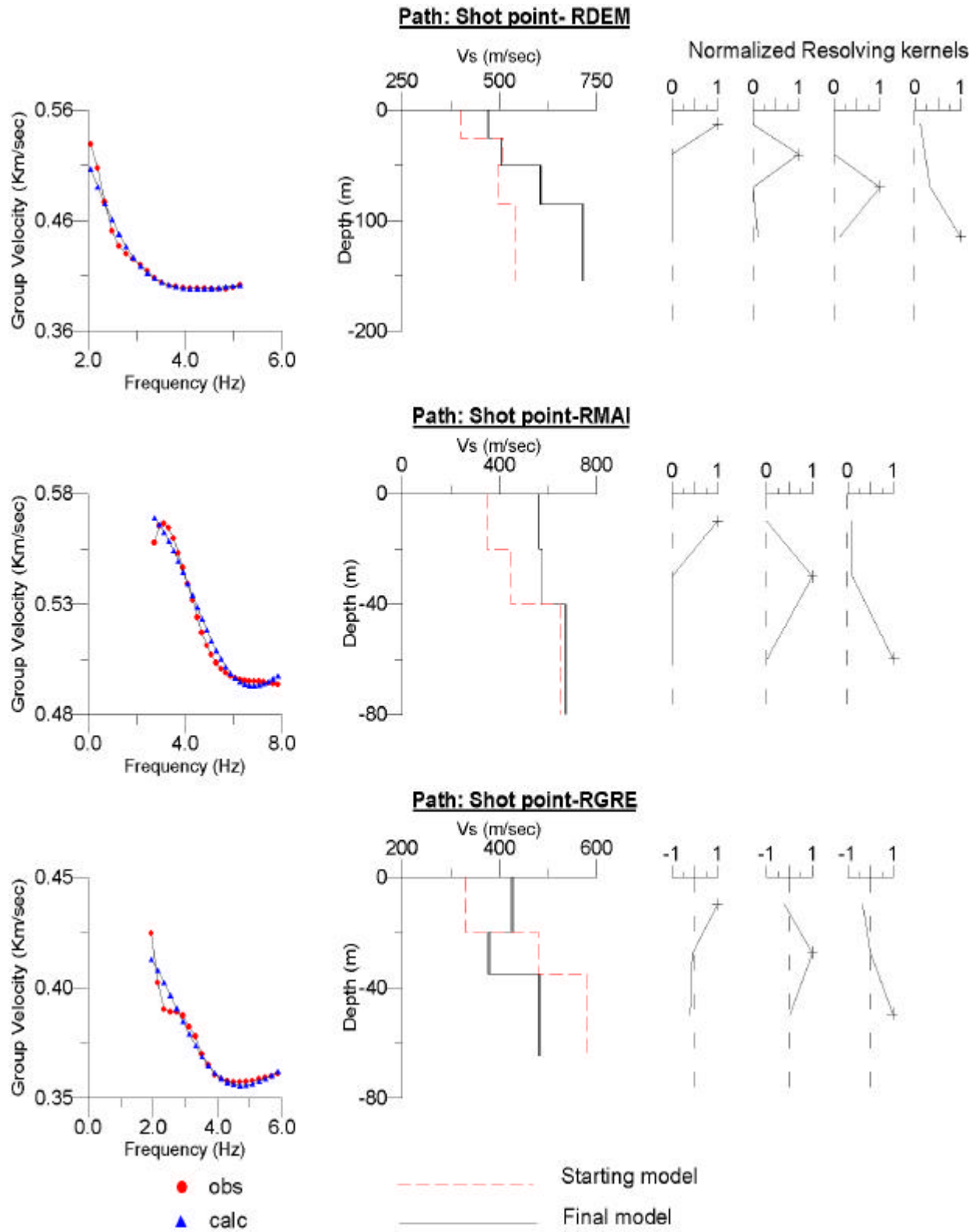
Stratigraphic sequence I: The velocities of shear waves in this sequence ranged between 370-430 m/sec, with an average thickness of 40-50 m.

Stratigraphic sequence II: The velocities of shear waves in this sequence ranged between 390-490 m/sec, with an average thickness of 50 m.
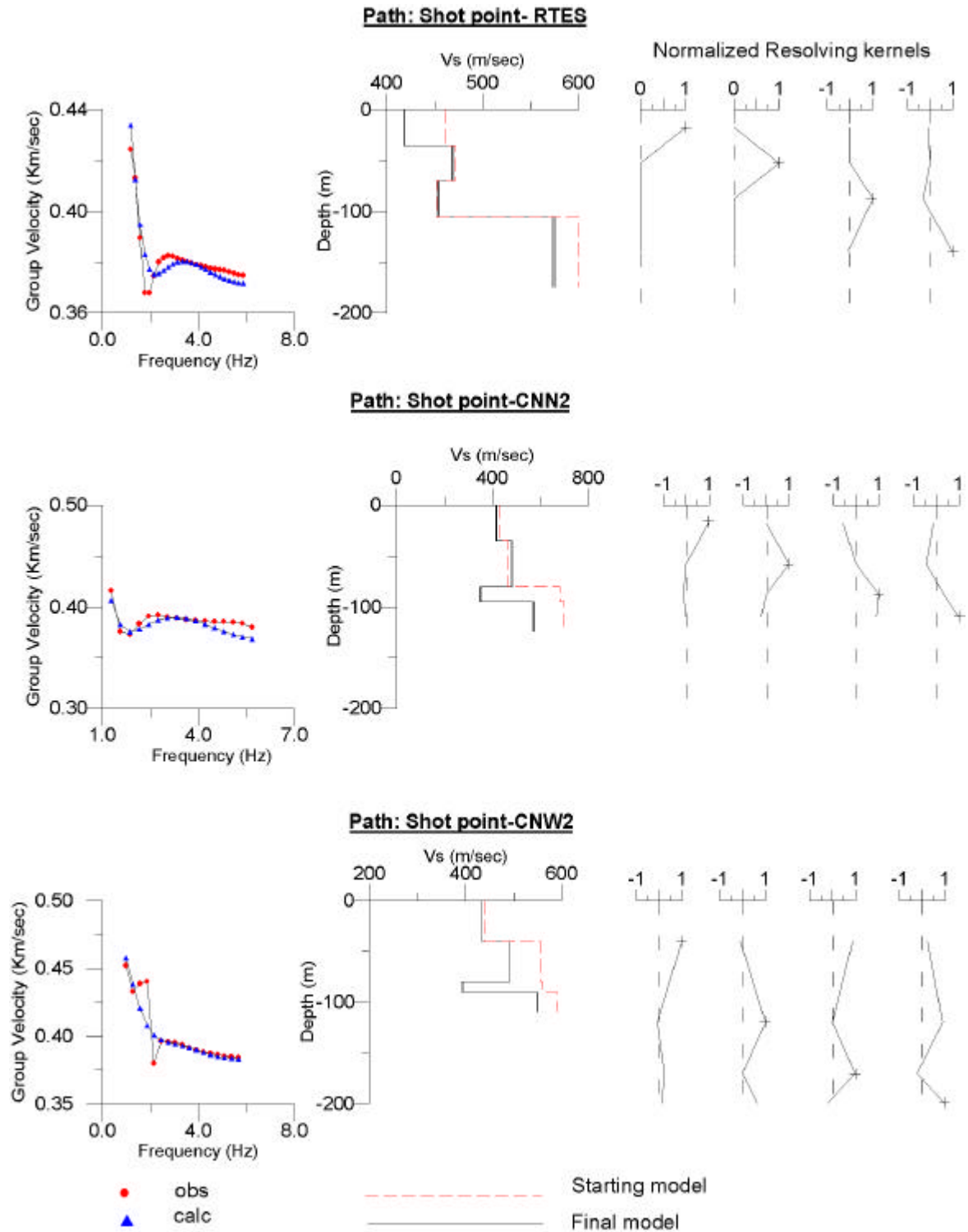
Stratigraphic sequence III: The velocities of shear waves in this sequence ranged between 470-720 m/sec.

The high velocities for the paths to RMAI and RDEM stations and the existence of the low velocities in the paths to RGRE and RTES stations can be explained as a flexure horst near the station RGRE. This assumption is in agreement with previous investigations, which were curried out in the Mygdonia basin (Final Scientific Report of Euro-seistest, 1995; Annual Scientific Report of Euro-seismod, 1997; Savvaidis *et al.*, 1997).
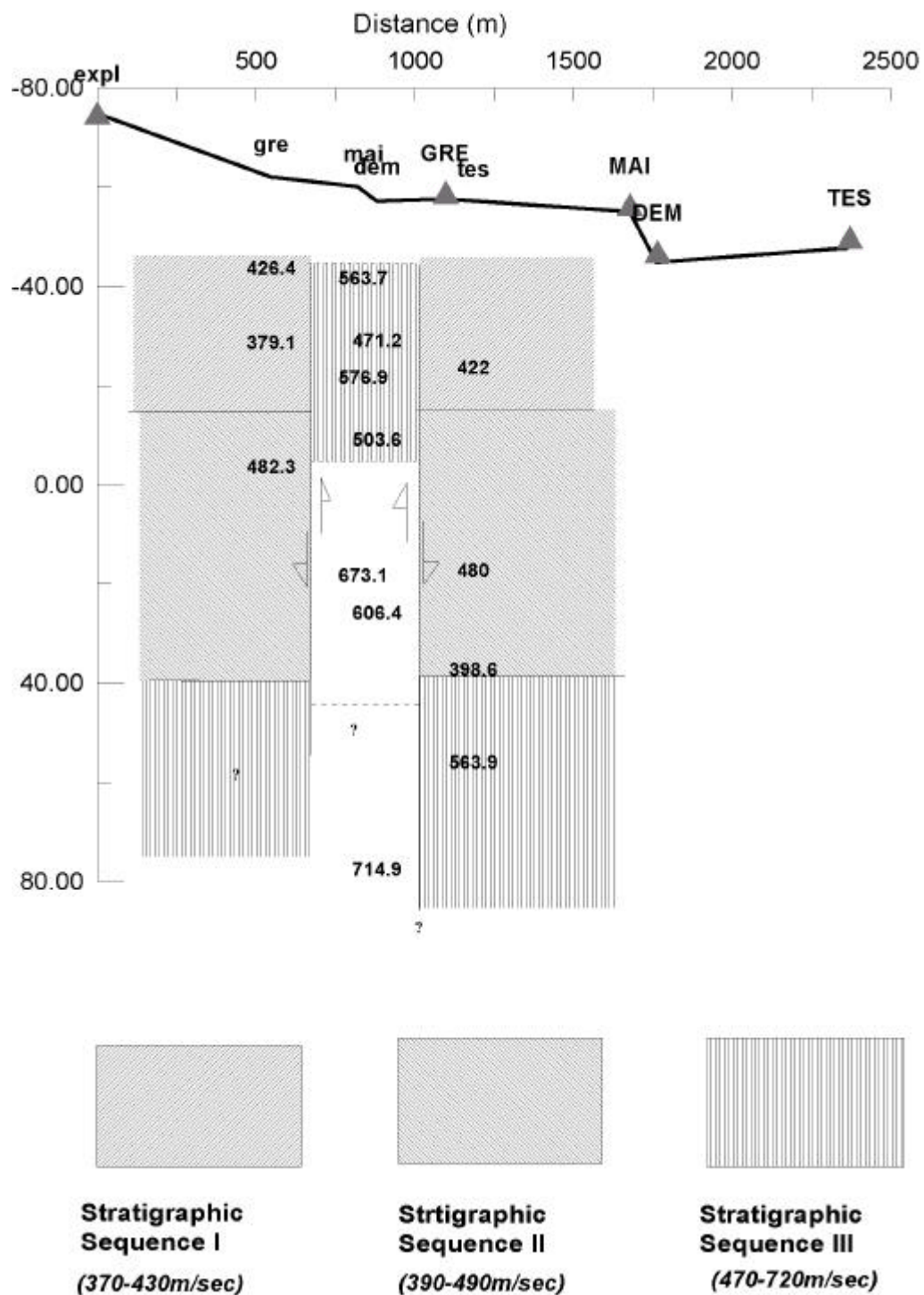
FIG. 6. Shear wave velocity versus depth profile, along the propagation path between shot point and Reftek stations. For each model the resolving kernels and the fit between observed and theoretical dispersion curves are presented.

FIG. 7. Shear wave velocity versus depth profile, along the propagation path between shot point and one Reftek station RTES, and two CIES stations CNN2, CNW2. For each model the resolving kernels and the fit between observed and theoretical dispersion curve are presented.

FIG. 8. Crustal structure of the very shallow layers along the profile of Reftek and Cies, in a NNW-SSE direction between the villages Profitis and Stivos. (The numbers are shear velocity in m/sec).

ACKNOWLEDGMENTS

REFERENCES

Backus, G., and Gilbert, F., 1967, Numerical application of a formalism for the geophysical inverse problems: Geophys. J. R. Astr. Soc., **13**, 247-276.

Backus, G., and Gilbert, F.,1968, The resolving power of gross Earth data: Geophys. J. Roy. Astr.Soc., **16**, 169-205.

Backus, G., and Gilbert, F., 1970, Uniqueness in the inversion of inaccurate gross earth data: Philos. Trans. R. Soc. Lond., Ser.A, **266**, 123-192.

Braile, L.W., and Keller, G.R., 1975, Fine structure of the crust, inferred from linear inversion of Rayleigh wave dispersion: Bull. Seism. Soc. Am., **65**, 71-83.

Burton, P.W., and Blamey, C., 1972, A computer program to determine the spectrum and a dispersion characteristic of transient signal.: HMSO, AWRE, Report No 0-48/72.

Dziewonski, A., Bloch, S., and Landisman, M., 1969, A technique for the analysis of transient seismic signals: Bull. Seism. Soc. Am., **59**, 427-444.

‘‘Euro-seismod, 1997’’. Development and Experimental Validation of Advanced Modelling Techniques in Engineering Seismology and Earthquake Engineering, (Commission of the European Communities), Annual report.

‘‘Euro-seistest, 1995’’. Volvi - Thessaloniki: A European Test Site for Engineering Seismology, Earthquake Engineering and Seismology, (Commis-sion of the European Communities), final scientific report, 600 p.

Faugeres, L., 1975, Recherches geomorphologi-ques en Grece septentrionale (Macedoine Central, Macedoine Occidentale).

Haskell, N.A., 1953, The dispersion of surface waves on multilayered media: Bull. Seism. Soc. Am., **43**, 17-34.

Jackson, D.D., 1972, Interpretation of inaccurate, insufficient and incosistent data: Geophys. J. R. Astr. Soc., **28**, 97-109.

Keller, G.R., Smith, R.B., Braile, L.W., Heaney, R., and Shurbet D.H., 1976, Upper crustal structure of the eastern Basin and Range, Northern Colorado Plateau and Middle Rocky Mountains from Rayleigh wave dispersion: Bull. Seism. Soc. Am., **66**, 869-876.

Koufos, G.D., Syrides, G.E., Kostopoulos, D.S., and Koliadimou, K.K., 1995, Preliminary results about the stratigraphy and the palaeonvironment of Mygdonia basin, Macedonia, Greece: Geobios., **18**, 243-249.

Lanczos, C., 1961, Linear differential operators, Van Nostrand (Eds), London.

Le Pichon, X., and Angelier J., 1979, The Hellenic arc and trench system: a key to the neotectonic evolution of the Eastern Mediterranean region: Tectonophys., **60**,1-42.

Levenberg, K., 1944, A method for the solution of certain non-linear problems in least squares: Quant. Appl. Math. **2**, 164-168.

Marquadt, D.W., 1963, An algorithm for least-squares estimation of non-linear parameters: J. Soc. Ind. Appl. Math.,. **11**, 431-441.

McKenzie, D.P., 1972, Active tectonics of the Mediterranean region: Geophys.J.R astr. Soc., **30**, 109-185.

McKenzie, D.P., 1978, Active tectonics of the Alpine-Himalayan belt : the Aegean Sea   and surrounding region: Geophys.J. R. astr. Soc., **55**, 217-254.

Mercier, J.L., 1977, Principal results of a neotectonic study of the Aegean arc and its localisation within the Eastern Mediterranean, VI Colloq. Aegean Region, Athens, 1281-1291.

Papazachos, B.C., and Comninakis, P.E., 1976, Modes of lithospheric interaction in the Aegean area: Intern. Symp. on the structural History of the Mediter. Region, Split (Yugoslavia), 25-29 October, 319-331.

Papazachos, B.C., Mountrakis, D., Psilovicos, A., and Leventakis G., 1980, Focal properties of the 1978 earthquakes in the Thessaloniki area: Bulgarian Geophys. J., **6**, 72-80.

Papazachos, B.C. , Kiratzi, A.A., Hatzidimitriou, P.M., and Rocca, A.C., 1984, Seismic faults in the Aegean area: Tectonophys., **106**, 71-85.

Paquin, C., Fridevaux, C., Bloyet, J., Ricard, Y., and Angelidis, C., 1981, Tectonic stresses on the mainland of Greece. In situ measurements by overcoring: Proc. of the Intern. Symp. on the Hell. Arc and Trench, Athens 1981, **2**, 88-103.

Psilovikos, A., 1977, Paleographic development of the basin and lake of Mygdonia (Langada-Volvi area, Greece): Ph.D. Thesis, University of Thessaloniki, 156 pp.

Psilovikos, A., and Sotiriadis L., 1983, The neotectonic graben complex of the Serbomacedonian massif at the area of Promygdinia basin, in northern Greece, Clausthaler Geol. Abh., **44**, 21-53.

Ritsema, A.R., 1974, The earthquake mechanism of the Balkan region: R. Netherl. Meteor. Inst. Rep., 74 -4, 1-36.

Savvaidis, A.S., Tsokas, G.N., and Pedersen, L.B., 1997, Crustal Structure of the Mygdonia Basin by MT Soundings: 29th General Assembly of the International Association of Seismology and Physics of the Earth's Interior (Abstract): Presented at The 29th General Assembly of the International Association of Seismology and Physics of the Earth's Interior (IASPEI), 18-28 August 1997, Thessaloniki., Greece.

Schwab, F.A., and Knopoff, L., 1972, Fast surface wave and free mode computations: In Methods in computational physics, Vol.II. Seismology: Surface waves and earth oscillations, 87-180, ed. Bolt, B.A., Academic Press, New york.

Scordilis, E. M., 1985, Microseismic study of the Servomacedonian zone and the surrounding area: Ph.D. Thesis, Univ. of Thessaloniki.

Smith, M.L., and Franklin, J.N., 1969, Geophysical application of generalised inverse theory: J. Geophys. Res., **74**, 2783-2785.

Soufleris, C., Jackson, A., King, G.C.P., Spencer C.P., and Scholz, C.H., 1982, The 1978 earthquake sequence near Thessaloniki, Northern Greece: Geophys. J. R. Astr. Soc., **68**, 429-458.

Thompson, W.T., 1950, Transmission of elastic waves through a stratified solid medium: J. Appl. Phys., **21**, 89-93.

Wiggins, R.A., 1972, The general linear inverse problem: Implications of surface waves and free oscillations for earth structure: Rev. Geophys. Space Phys., **10**, 251-285.